APPLICATION OF SYMMETRIES IN THREE-DIMENSIONAL HEXAGONAL-Z NODAL DIFFUSION CALCULATION

Shaohong Zhang and Zhongsheng Xie
Department of Nuclear Engineering
Xian Jiaotong University
Xian, Shaanxi 710049, P. R. China
shzhang@xanet.edu.cn; zsxie@xjtu.edu.cn

ABSTRACT

The symmetries have been successfully applied to two-dimensional hexagonal nodal diffusion calculation. In the two-dimensional diffusion code GTDIF-H, a first-order partial current moment nodal boundary condition has been introduced to improve the nodal solution and satisfactory results have been achieved for various benchmark problems. In this paper, the method is extended to three-dimensional hexagonal-z geometry. Based on the extended methodology, a new three-dimensional multigroup diffusion code GT3D-H is developed and successfully verified by the WWER benchmark problems.

1. INTRODUCTION

In reference 1, a new two-dimensional hexagonal nodal method based on the analytic representation of intronodal flux distribution and the symmetries of a hexagon has been proposed. The method has demonstrated several advantages. Firstly, it directly solves the multidimensional diffusion equation rather than a set of transversely integrated equations, thus it avoids the need of approximation of transverse leakage shape and the difficulty caused by the singular terms occurring in the procedure of transverse integration in the hexagonal geometry. Secondly, by introducing a first-order partial current moment in the nodal coupling, it enables the full representation of the symmetries of the intranodal flux. Numerical results of a series of benchmark problems demonstrate that the method is very accurate for prediction of criticality and power distribution. Its accuracy is comparable to that of ANC-H[2-3] for the benchmark problems presented in reference 3. This paper extends the two-dimensional code GTDIF-H[1] to three dimensions. As a result, a three-dimensional multigroup hexagonal nodal diffusion code GT3D-H has been developed and successfully verified by the WWER benchmark problems.

2. NODAL METHOD FORMALISM

2.1 ANALYTIC NODAL FLUX REPRESENTATION

Consider the following matrix form of G groups neutron diffusion equation in a conventional homogenous hexagonal prism (node):

$$-\mathbf{D}\nabla^2 \boldsymbol{F}(\boldsymbol{r}) + \mathbf{S}(k_{eff})\boldsymbol{F}(\boldsymbol{r}) = \boldsymbol{0} \tag{1}$$

with **D** being a diagonal matrix of diffusion constants and **S** a energy transfer matrix of order G. Eq(1) can be transformed to the vector Helmholtz equation and the general solution of nodal flux can be expressed in its component form as[4-5]

$$\boldsymbol{F}_g(\boldsymbol{r}) = \sum_{i=1}^{G} \mathbf{U}_{gi} \int_{|\boldsymbol{w}|=1} C_i(\boldsymbol{w}) \exp(\boldsymbol{l}_i \boldsymbol{w}\boldsymbol{r}) d\boldsymbol{w} \qquad g = 1,2,\cdots,G \tag{2}$$

where the inner production $\boldsymbol{w}\boldsymbol{r} = w_1 x + w_2 y + w_3 z$, $w_1^2 + w_2^2 + w_3^2 = 1$. The matrix **U** and parameters $\boldsymbol{l}_i$ are determined by the following matrix eigenvalue problem

$$\mathbf{D}^{-1}\mathbf{S}\mathbf{U} = \mathbf{U}\,\underset{i=1,G}{diag}(\boldsymbol{l}_i^2) \tag{3}$$

$C_i(\boldsymbol{w})$ in Eq(2) are unknown functions needed to be determined from the following nodal boundary conditions

$$\boldsymbol{B}_{gs}^{-}\boldsymbol{F}_g(\boldsymbol{r}) \equiv \left[\frac{1}{4}\boldsymbol{F}_g(\boldsymbol{r}) + \frac{D_g}{2}\frac{d}{d\boldsymbol{n}_s}\boldsymbol{F}_g(\boldsymbol{r})\right]_{\boldsymbol{r}\in F_s} = J_{gs}^{-}(\boldsymbol{r}_s) \tag{4}$$

where F_s is the s-th surface of the hexagonal node, $s = 1,2,\cdots,8$ with $s = 1,2,\cdots,6$ numbering the radial nodal surfaces and 7 for the top surface and 8 for the bottom surface. $\boldsymbol{n}_s$ is the unit out-going normal vector of F_s. $J_{gs}^{-}(\boldsymbol{r}_s)$ is the entering partial current at the s-th nodal surface.

The analytic nodal solution satisfies Eq(1) at any point in the nodal region. However, the unknown functions $C_i(\boldsymbol{w})$ are difficult to be determined by a straightforward application of Eq(2) to Eq(4). Moreover, the response relationships between the entering and out-going currents are difficult to be obtained from Eq(4). It will be illustrated in the following sections that the difficulty can be greatly reduced when the symmetries are employed in the nodal method formalism.

2.2 FORMULTAION OF THE BOUNDARY PROBLEM FOR THE IRREDUCIBLE COMPONENTS OF NODAL FLUX

Any hexagonal node has a certain type of symmetry and it is described by D_{6h} group for the three-dimensional hexagonal prism geometry. From group theory we learn that any function can be decomposed into its irreducible or symmetry components (i.e. projections in basis vectors of subspaces transformed by irreducible representation of the group D_{6h}) and each component is linearly independent to the others. Furthermore, since each component is an eigenfunction of the symmetries, it is sufficient to determine each symmetry component on a part of hexagonal node and the solution can be unfolded to the whole node by applying the symmetries. Therefore it is convenient to solve the problems of symmetry components of the intranodal flux in stead of the original problem Eq(1) and Eq(4).

By applying the projecting operator[5] that projects an arbitrary function in the basis vectors of irreducible subspaces of D_{6h} group, we can obtain the kth symmetry component of intranodal flux as follows:

$$\boldsymbol{F}_{gk}(\boldsymbol{r}) = \sum_{i=1}^{G} \mathbf{U}_{gi} \int_{|\boldsymbol{w}|=1} C_{ik}(\boldsymbol{w}) \exp_k(\boldsymbol{l}_i \boldsymbol{w}\boldsymbol{r}) \mathrm{d}\boldsymbol{w} \quad k = 1,2,\cdots,K \tag{5}$$

Here functions $C_{ik}(\boldsymbol{w})$ and $\exp_k(\boldsymbol{l}_i \boldsymbol{w}\boldsymbol{r})$ are the kth symmetry component of function $C_i(\boldsymbol{w})$ and $\exp(\boldsymbol{l}_i \boldsymbol{w}\boldsymbol{r})$ respectively and K is the total number of basis vectors that span each irreducible representation subspaces of the symmetry group. It can be derived from the group theory that for the D_{6h} group, K=16, while for the C_{6v} group of the symmetries of a two-dimensional hexagon, K=8. The three-dimensional intranodal flux distribution is the sum of all its 16 symmetry components:

$$\boldsymbol{F}_g(\boldsymbol{r}) = \sum_{k=1}^{16} \boldsymbol{F}_{gk}(\boldsymbol{r}) \tag{6}$$

It is easy to verify that each $\boldsymbol{F}_{gk}(\boldsymbol{r})$ defined in Eq(5) satisfies the nodal diffusion equation Eq(1). Substituting Eq(6) into Eq(4), the nodal surface entering partial current can also be decomposed into its symmetry components. From the linear independency of symmetry component, the nodal boundary condition for the kth symmetry component $\boldsymbol{F}_{gk}(\boldsymbol{r})$ can be derived as follows:

$$\boldsymbol{B}_{gs}^{-} \boldsymbol{F}_{gk}(\boldsymbol{r}) = J_{gsk}^{-}(\boldsymbol{r}_s) \tag{7}$$

Here J_{gsk}^{-} is the kth component of entering partial current at the sth nodal surface.

Instead of solving the original problem Eq(1) and Eq(4), now 16 sets of Eq(5) and Eq(7) for symmetry components will be solved. Since each component has a certain type of symmetry, the solution of Eq(5) and Eq(7) is much easier than that of Eq(1) and Eq(4).

2.3 SYMMETRIES OF IRREDUCIBLE COMPONENTS AND THE IMPROVEMENT OF NODAL BOUNDARY CONDITION

In reference 1, the defect of the face-averaged nodal boundary condition has been pointed out from the symmetry point of view. We have improved the nodal coupling and the accuracy of the nodal solution by the introduction of the first-order partial current moment boundary condition. In this section, the symmetries of irreducible components will be analyzed and the first-order partial current moment nodal boundary condition will be extended to its three-dimensional application.

To illustrate the symmetries of irreducible components, let us consider an arbitrary point $\boldsymbol{r}_0$ in the nodal region. By performing all the symmetry transformations (rotation and reflection etc.) of a hexagonal prism, 24 symmetry points of $\boldsymbol{r}_0$ will be generally obtained. By comparing the function values of $\boldsymbol{F}_{gk}(\boldsymbol{r})$ at these symmetry points, the symmetry properties of each component will be found out. For example, for the first symmetry component $\boldsymbol{F}_{g1}(\boldsymbol{r})$, we have

$$\boldsymbol{F}_{g1}(\boldsymbol{r}_0) = \boldsymbol{F}_{g1}(\boldsymbol{r}_i), \quad i = 1,2\cdots 23 \tag{8}$$

Namely, the function values of the first symmetry component at these symmetry points are all the same, while for $k = 2,3,4$, the symmetries of each component are illustrated in Table I.

Table I. Symmetry Properties of the Irreducible Components of $F_g(r)$

Components		Symmetry Points Distribution[a]											
		-30° ~0°	0° ~30°	30° ~60°	60° ~90°	90° ~120°	120° ~150°	150° ~180°	180° ~-150°	-150° ~-120°	-120° ~-90°	-90° ~-60°	-60° ~-30°
k=2	U	–	+	–	+	–	+	–	+	–	+	–	+
	L	–	+	–	+	–	+	–	+	–	+	–	+
k=3	U	+	+	–	–	+	+	–	–	+	+	–	–
	L	–	–	+	+	–	–	+	+	–	–	+	+
k=4	U	–	+	+	–	–	+	+	–	–	+	+	–
	L	+	–	–	+	+	–	–	+	+	–	–	+

[a] The angle is counted from the direction of the unit out-going normal vector of one nodal surface.

Here U and L mean the upper and lower halves of the nodal height respectively. The symmetry properties for other irreducible components can also be analyzed. Limited by the paper length, they are not fully presented here.

From Table I it is obvious that if we define the face-averaged nodal boundary condition for $\boldsymbol{F}_{gk}(\boldsymbol{r})$ as

$$\frac{1}{F_s}\int_{F_s} \boldsymbol{B}^{-}_{gs}\boldsymbol{F}_{gk}(\boldsymbol{r})d\boldsymbol{r}_s = \frac{1}{F_s}\int_{F_s} J^{-}_{gsk}(\boldsymbol{r}_s)d\boldsymbol{r}_s = \bar{J}^{-}_{gsk} \tag{9}$$

then the right-hand side of Eq(9) equals zero for k=2,3 and 4. That means these components have no contribution to the face-averaged parameters and one can not expect to consider the effects of these components from the given face-averaged entering partial currents. There are 9 components in total whose face integration equals zero.

Apparently, other nodal boundary conditions should be provided for the full representation of these irreducible components. There are several options for the choices of the additional boundary conditions. In reference 1, a new type of boundary condition that simultaneously requires the continuity of both the zero- and first-order partial current moments across the nodal surfaces was proposed which enabled the full representation of the symmetries of a hexagon and significantly improved the accuracy of the nodal solution. While for the three-dimensional hexagonal-z problem, it can be seen from Table I that the additional boundary condition of continuity of first-order partial current moment with weighted sign function is still can be used to represent the antisymmetric components in the radial plane. Therefor, it can be extended to three dimensions and used as an additional nodal boundary condition in the radial nodal coupling. Thus, at each radial nodal surface, two boundary conditions exist for the symmetry components of nodal flux, namely

$$\begin{aligned}
&\frac{1}{F_s}\int_{F_s} \boldsymbol{B}^{-}_{gs}\boldsymbol{F}_{gk}(r)d\boldsymbol{r}_s = \bar{J}^{-}_{gsk} \\
&\frac{1}{F_s}\int_{F_s} \mathrm{sgn}(\boldsymbol{r}_s)\boldsymbol{B}^{-}_{gs}\boldsymbol{F}_{gk}(r)d\boldsymbol{r}_s = \bar{J}^{1,-}_{gsk}, \quad s = 1,2,\cdots,6
\end{aligned} \tag{10}$$

While in the axial direction only the face-averaged nodal boundary condition is used since it is too complicate to define a similar first-order partial current nodal boundary condition.

After the introduction of the first-order partial current moment in the radial nodal coupling, a better representation of the symmetries of the nodal flux can be achieved and more nonzero irreducible components will be presented in the expression of intranodal flux. It will be demonstrated in Section 3 that the radial nodal power distribution will be considerably improved because of the improvement of the nodal coupling and better representation of symmetries in the radial plane.

2.4. NUMERICAL IMPLEMENTATION

For numerical solution of Eq(5) and Eq(10), a proper approximation of $C_i(\boldsymbol{w})$ needs to be introduced. Here, we express $C_i(\boldsymbol{w})$ function as a sum of 14 delta functions

$$C_i(\boldsymbol{w}) = \sum_{n=1}^{14} d_{in}\boldsymbol{d}(\boldsymbol{w} - \boldsymbol{w}_n) \tag{11}$$

where $\boldsymbol{w}_n$, $n = 1,\cdots,12$ are a group of symmetry points distributed on the equator of the unit sphere of vector $\boldsymbol{w}$, the distribution of $\boldsymbol{w}_n$ is given in detail in reference 1. While $\boldsymbol{w}_{13}$ and $\boldsymbol{w}_{14}$ are two unit vectors distributed symmetrically on the polar axis of the unit sphere.

Based on the representation of Eq(11), each irreducible component of $C_i(\boldsymbol{w})$ function can be derived from its projection decomposition. And the irreducible components of $\exp(\boldsymbol{l}_i\boldsymbol{w}\boldsymbol{r})$ can also be explicitly expressed by hyperbolic, trigonometric, or a combination of both functions. Substituting both expressions into Eq(5), the integration over $\boldsymbol{w}$ is discretized as a sum of function values of $C_{ik}(\boldsymbol{w})$ and $\exp_k(\boldsymbol{l}_i\boldsymbol{w}\boldsymbol{r})$ at the points of $\boldsymbol{w}_n$. Here we can utilize the symmetry properties of $C_{ik}(\boldsymbol{w})$ and $\exp_k(\boldsymbol{l}_i\boldsymbol{w}\boldsymbol{r})$ to simplify the expression of $\boldsymbol{F}_{gk}(\boldsymbol{r})$. Substituting the resulted expressions of $\boldsymbol{F}_{gk}(\boldsymbol{r})$ into Eq(10), we could determine the unknown function values of $C_{ik}(\boldsymbol{w}_n)$ from the respective symmetry component of nodal entering current moments, then the symmetry components $\boldsymbol{F}_{gk}(\boldsymbol{r})$ could be uniquely determined. Once we have solved these components, the symmetry components of nodal out-going partial current moments could easily be derived from the Fick's law. Eliminate the parameters $C_{ik}(\boldsymbol{w}_n)$ in the expressions of the symmetry components of entering and out-going partial current moments, the nodal response relationships between the symmetry components of entering and out-going partial current moments can be derived. The resulted nodal response matrix equations are illustrated as follows:

$$\begin{aligned}
\boldsymbol{I}_1^{+} &= \mathbf{R}_1\boldsymbol{I}_1^{-} \\
\boldsymbol{I}_2^{1,+} &= \mathbf{R}_2\boldsymbol{I}_2^{1,-} \\
\boldsymbol{I}_3^{1,+} &= \mathbf{R}_3\boldsymbol{I}_3^{1,-} \\
\boldsymbol{I}_4^{0,+} &= \mathbf{R}_4\boldsymbol{I}_4^{0,-} \\
&\vdots
\end{aligned} \tag{12}$$

where $\boldsymbol{I}_k^{0,-}$ and $\boldsymbol{I}_k^{1,-}$ are column vectors related to the kth component of zero- and first-order moment of entering partial current respectively

$$\begin{aligned}
\boldsymbol{I}_k^{0,-} &= col(a_{1k},\cdots,a_{gk},\cdots,a_{Gk}) \\
\boldsymbol{I}_k^{1,-} &= col(a_{1k}^1,\cdots,a_{gk}^1,\cdots,a_{Gk}^1)
\end{aligned} \tag{13}$$

a_{gk} and a_{gk}^1 are parameters determined from the linear combination of the zero- and first-order moment of entering currents at six nodal surfaces, for instant

$$a_{g1} = \frac{1}{6}(\bar{J}^{-}_{g1} + \bar{J}^{-}_{g2} + \bar{J}^{-}_{g3} + \bar{J}^{-}_{g4} + \bar{J}^{-}_{g5} + \bar{J}^{-}_{g6})$$
$$a^{1}_{g2} = \frac{1}{6}(\bar{J}^{1,-}_{g1} + \bar{J}^{1,-}_{g2} + \bar{J}^{1,-}_{g3} + \bar{J}^{1,-}_{g4} + \bar{J}^{1,-}_{g5} + \bar{J}^{1,-}_{g6}) \quad (14)$$

Where $\bar{J}^{-}_{gs}$ and $\bar{J}^{1,-}_{gs}$ are the face-averaged entering partial current and first-order entering partial current moment at the sth nodal surface respectively.

While vectors $\boldsymbol{I}^{0,+}_{k}$ and $\boldsymbol{I}^{1,+}_{k}$ are the counterparts of $\boldsymbol{I}^{0,-}_{k}$ and $\boldsymbol{I}^{1,-}_{k}$ for the out-going partial current moments. $\boldsymbol{I}^{\pm}_{1} = col(\boldsymbol{I}^{0,\pm}_{1}, \boldsymbol{I}^{\pm}_{1,z})$ and $\boldsymbol{I}^{\pm}_{1,z} = col(a^{\pm}_{11,z}, \cdots, a^{\pm}_{g1,z}, \cdots, a^{\pm}_{G1,z})$. The parameters $a^{\pm}_{g1,z}$ are determined from the linear combination of the nodal entering or out-going partial currents at the axial direction. The response matrices **R**s are determined from the geometry and nuclear parameters of the node.

To obtain the core multiplication factor, the equation for nodal averaged flux should be founded. Since the irreducible components of intranodal flux have been determined in the procedure of deriving the nodal response matrixes, the nodal averaged flux can be calculated from the resulted analytic representation of intranodal flux distribution. Only the first component of intranodal flux will remain in the expression of nodal averaged flux and therefore the nodal averaged flux can be determined from the first component of the nodal entering partial currents as follows:

$$\overline{\boldsymbol{\mu}} = \mathbf{R}_0 \boldsymbol{I}^{-}_{1} \quad (15)$$

where matrix $\mathbf{R}_0$ is also determined from the geometry and nuclear parameters of the node.

3. NUMERICAL VERIVIFATION

Based on the proposed method, a three-dimensional multigroup hexagonal-z nodal diffusion code GT3D-H is developed. To demonstrate the effect of the introduction of continuity of first-order partial current moment in the radial nodal boundary condition, a three-dimensional code GT3D-H0 is also developed in which only the face-averaged nodal boundary condition is employed. Both methods are verified against the three-dimensional WWER-440 and WWER-1000 benchmark problems[3]. Table II presents the summary of the numerical results for WWER-440 problem, where the $\boldsymbol{e}_{\max}$ and $\bar{\boldsymbol{e}}$ are the maximum and mean percentage errors of nodal power density respectively, $\boldsymbol{e}_{\boldsymbol{k}}$ is the error in pcm of $k_{\boldsymbol{eff}}$. The nodal code NDHEX[6] is very similar to the DIF3D-N[7]. Table III gives the comparison of the results for the WWER-1000 benchmark problem, where the $\boldsymbol{e}_{\max}$ means the maximum percentage error of the collapsed assembly power density of upper and lower halves of the core. Figure 1 and 2 illustrate the power density distribution of upper and lower halves core obtained by GT3D-H and SIXTUS-3 respectively.

Table II. Summary of Numerical Results for the WWER-440 Benchmark Problem.

Code Option	Two-dimensional			Three-dimensional			Three-dimensional collapsed radial distribution	Three-dimensional collapsed axial distribution
	ε_k	ε_{max}	$\bar{\varepsilon}$	ε_k	ε_{max}	$\bar{\varepsilon}$	ε_{max}	ε_{max}
GT3D-H	-7.0	0.48	0.18	34	-3.52	0.87	-0.92	-2.49
ANC-H	37	0.82	-	25	1.28	-	1.00	0.66
GT3D-H0	51.9	-1.20	0.58	72	-3.09	1.10	-2.45	-1.39
SIXTUS2/3[8-9]	42.6	-0.88	0.42	58	-5.89	1.60	-2.60	-3.63
NDHEX	-166.3	9.50	3.63	4	8.74	3.02	-6.78	-0.34

Table III. Summary of Numerical Results for the WWER-1000 Benchmark Problem.

Code Option	GT3D-H	ANC-H	GT3D-H0	SIXTUS-3	DIF3D-N
ε_k	29.4	13.0	62.7	62.1	7.0
ε_{max}	-1.33	0.9	3.36	3.39	4.4

The results of the WWER benchmark problems demonstrate that the proposed method is an accurate and efficient method for predicting the criticality and nodal power distribution in the hexagonal-z geometry. Its accuracy is comparable and close to that of ANC-H and is better than that of SIXTUS-3 and DIF3D-N. Table II also indicates that after the introduction of the first-order partial current moment nodal coupling in the radial plane, the core radial power distribution has been apparently improved. The axial power distribution remains unimproved due to the simple nodal coupling that is employed. A further seeking of a better axial nodal coupling is now undertaking by authors.

CONCLUSIONS

A new three-dimensional hexagonal nodal method that exploits the symmetries is described. By introducing the first-order partial current moment in the nodal formalism the new method achieves a full representation of the symmetries of the intranodal analytic solution in the radial plane, both the symmetric and asymmetric irreducible components of the nodal flux are represented. Based on the proposed nodal theory, a three-dimensional multigroup hexagonal-z diffusion code GT3D-H is developed and successfully tested by the WWER Benchmark problems.

REFERENCES

1. Shaohong Zhang, Zhongsheng Xie, "A New Nodal Method Based on Group Theory for the Multigroup Diffusion Calculation in Hexagonal Geometry," Proceedings of International Conference on the Physics of Nuclear Science and Technology, Long Island, New York, Oct. 5-8, 1998, pp. 986-993.

2. Y. A. Chao, N. Tsoulfanidis, "Conformal Mapping and Hexagonal Nodal Methods—I: Mathematical Foundation," *Nucl. Sci. & Eng.*, **121**, pp. 202-209 (1995).

3. Y. A. Chao, Y. A. Shatilla, "Conformal Mapping and Hexagonal Nodal Methods—II: Implementation in the ANC-H Code," *Nucl. Sci. & Eng.*, **121**, pp. 210-225 (1995).

4. Makai Mihaly, "Symmetries Applied to Reactor Calculations," *Nucl. Sci. & Eng.*, **82**, pp. 338-353 (1982).

5. O. G. Komlev, "A Group Theory Nodal Method for the Diffusion Equation in 3-D Hexagonal Geometry," Proceedings of International Conference on the Physics of Reactors, Mito, Japan, Sept. 16-20, 1996, pp. A-60-69.

6. Kan Wang, Zhongsheng Xie, "NDHEX - A Program for Three Dimensional Nodal Diffusion Theory Calculation in HEX-Z Geometry," *Chinese Journal of Nuclear Power Engineering*, **14,** pp. 326-334 (1993).

7. R. D. Lawrence, "The DIF3D Nodal Neutronics Option for Two- and Three-dimensional Diffusion Theory Calculation in Hexagonal Geometry," ANL-83-1, Argonne National Laboratory (Mar. 1983).

8. J. J. Arkuszewski, "SIXTUS-2: A Two-dimensional Multigroup Diffusion Code in Hexagonal Geometry," *Progress in Nuclear Energy*, **18**, pp. 123-136 (1986).

9. J. J. Arkuszewski, Y. Kawagoe and T. Takeda, "SIXTUS-3: A Three-dimensional Nodal Diffusion Code in Hex-Z Geomery," PSI-Bericht Nr. 102 (1991).

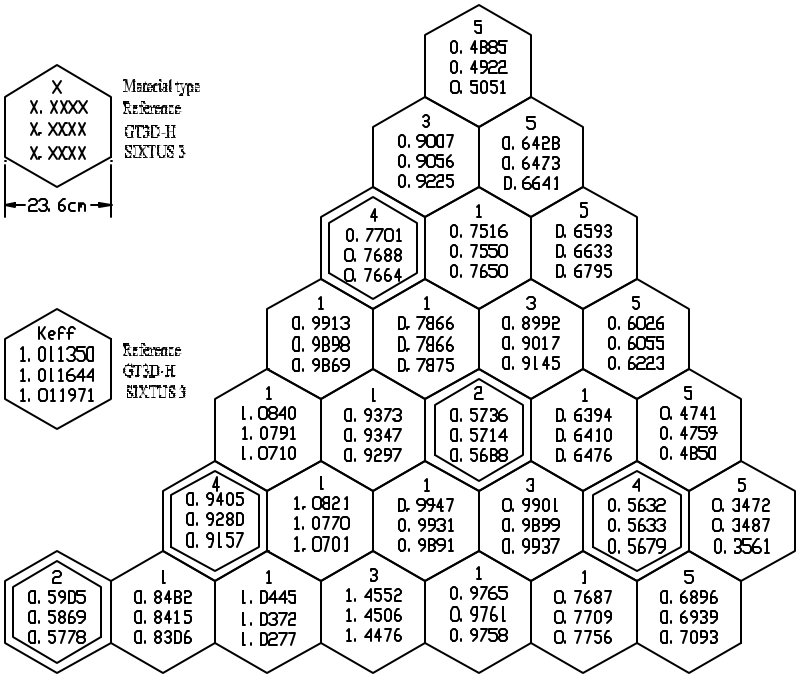

Figure 1. Radial power density distribution on upper core of the WWER-1000 problem.

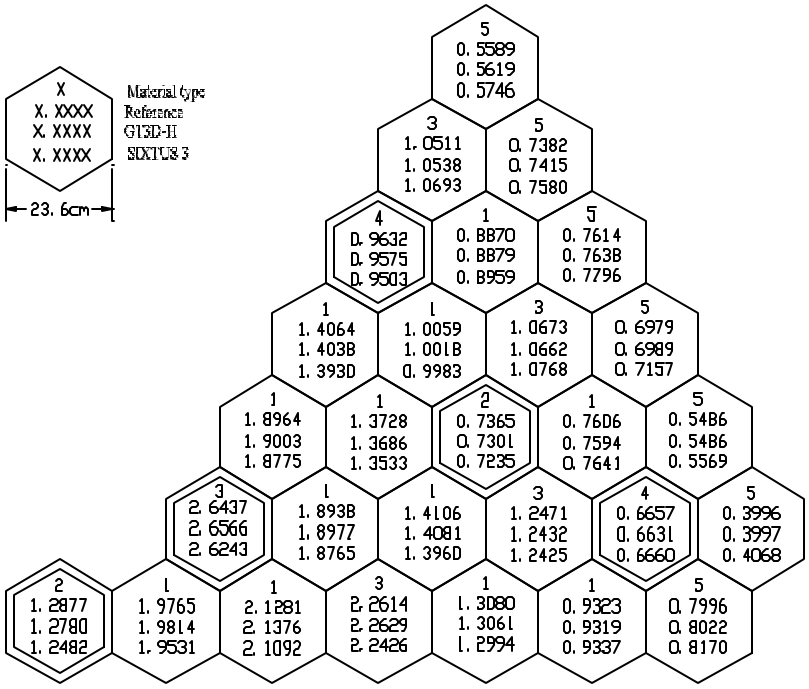

Figure 2. Radial power density distribution on lower core of the WWER-1000 problem.